JACS
JOURNAL OF THE AMERICAN CHEMICAL SOCIETY
pubs.acs.org/JACS
Article

Observation of a Symmetry-Forbidden Excited Quadrupole-Bound State

Yuan Liu, Guo-Zhu Zhu, Dao-Fu Yuan, Chen-Hui Qian, Yue-Rou Zhang, Brenda M. Rubenstein, and Lai-Sheng Wang*

Cite This: https://dx.doi.org/10.1021/jacs.0c10552
Read Online

ABSTRACT: We report the observation of a symmetry-forbidden excited quadrupole-bound state (QBS) in the tetracyanobenzene anion ($TCNB^-$) using both photoelectron and photodetachment spectroscopies of cryogenically-cooled anions. The electron affinity of TCNB is accurately measured as 2.4695 eV. Photodetachment spectroscopy of $TCNB^-$ reveals selected symmetry-allowed vibronic transitions to the QBS, but the ground vibrational state was not observed because the transition from the ground state of $TCNB^-$ (A_u symmetry) to the QBS (A_g symmetry) is triply forbidden by the electric and magnetic dipoles and the electric quadrupole. The binding energy of the QBS is found to be 0.2206 eV, which is unusually large due to strong correlation and polarization effects. A centrifugal barrier is observed for near-threshold autodetachment, as well as relaxations from the QBS vibronic levels to the ground and a valence excited state of $TCNB^-$. The current study shows a rare example where symmetry selection rules, rather than the Franck–Condon principle, govern vibronic transitions to a nonvalence state in an anion.

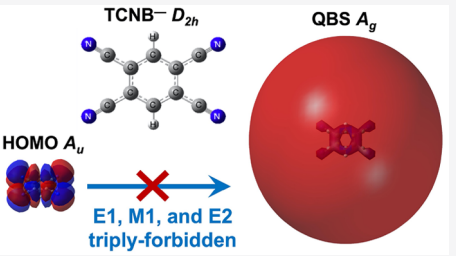

INTRODUCTION

Fermi and Teller first derived a critical value of 1.625 D for a point dipole to bind an electron.[1] This value was later rederived by several investigators, as outlined in an interesting account by Turner.[2] For a realistic molecular system to support a diffuse dipole-bound state (DBS), the critical dipole moment has been determined empirically to be ~2.5 D.[3−8] Dipole-bound anions have been formed by Rydberg electron transfer (RET)[3−6,9] for polar neutral molecules that do not form valence anions. Stable valence-bound anions with polar neutral cores can support dipole-bound excited states just below the electron detachment threshold.[10−12] DBSs as a special class of electronically excited states of valence-bound anions have allowed the observations of vibrational mode-specific autodetachment and the realization of resonant photoelectron spectroscopy (rPES),[13−16] which yields much richer spectroscopic information than conventional anion PES for relatively complicated molecular systems. Dipole-bound states in simpler molecular anions including diatomic species have been observed recently.[17−20] The autodetachment lifetimes from different vibrational levels of the excited DBS of the phenoxide anion have been directly measured using a pump–probe technique in a very recent study.[21]

Nonpolar neutral molecules can bind an electron via their quadrupolar potential ($-1/r^3$) and form quadrupole-bound anions.[22−27] Critical quadrupole moments were studied for a quadrupole-bound state (QBS),[24−27] but ab initio calculations indicated that a critical quadrupole moment does not exist because of the complexity of the molecular interactions and strong electron correlation effects.[28] Since the first suggestion of the rhombic $(BeO)_2^-$ as a quadrupole-bound anion,[29] the rhombic alkali halide dimers[30,31] and several organic molecules[28] with vanishing dipole moments were proposed to be targets for quadrupole-bound anions, and the rhombic $(MgO)_2^-$ was studied by PES.[32] The CS_2^- anion formed via RET was initially suggested to be quadrupole-bound.[33,34] Quadrupole-bound anions were observed for the formamide dimer and *para*-dinitrobenzene[35,36] and *trans*-succinonitrile.[37,38] Recently, RET in combination with PES has allowed the binding energies of two quadrupole-bound anions to be convincingly determined.[39,40] Similar to excited DBSs, the neutral core of a valence-bound anion with a vanishing dipole moment but a large quadrupole moment can support an excited QBS below the electron detachment threshold. An excited QBS has been observed in the 4-cyanophenoxide anion[41] because neutral 4-cyanophenoxy has a very small dipole moment of 0.3 D but a large quadrupole moment. However, excited QBS supported by a quadrupolar field without any residual dipole moment has not been observed. Such a highly-symmetric QBS may reveal additional

Received: October 9, 2020

https://dx.doi.org/10.1021/jacs.0c10552
J. Am. Chem. Soc. XXXX, XXX, XXX−XXX

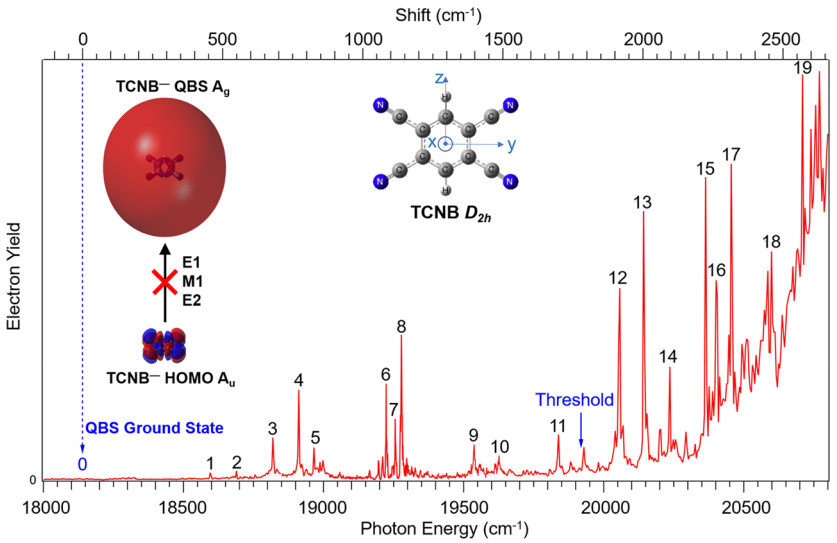

Figure 1. Photodetachment spectrum of $TCNB^-$ obtained by monitoring the electron yield as a function of photon energy. Resonant peaks are labeled as 1−19 corresponding to vibrational levels of the QBS. Note the 0−0 transition from the anion ground state (A_u) to the QBS (A_g) is E1, M1, and E2 triply forbidden. It is deduced to be at an excitation energy of 18 139 cm^{-1} indicated by the dashed arrow and labeled as 0 (see text). The detachment threshold at 19 918 cm^{-1} is indicated by a short arrow. The molecular structure of TCNB (D_{2h}) and the associated coordinates are given in the inset. The HOMO of $TCNB^-$ and the QBS (plotted with an isovalue of 0.0004) are also given in the inset. Note the σ-like symmetry and the diffuseness of the QBS orbital.

information about the role that symmetry plays in these diffuse electronic states near the detachment threshold.

In this article, we report the observation of such an excited QBS in the 1,2,4,5-tetracyanobenzene anion ($TCNB^-$) cryogenically cooled to its vibrational ground state. The neutral TCNB molecule containing four polar −CN groups[42] is a good electron acceptor and can form a stable valence-bound anion.[43,44] Owing to its high symmetry (D_{2h}, see inset of Figure 1), TCNB has no dipole or octupole moments but a large quadrupole moment with only nonzero diagonal terms (Q_{xx} = 19.3, Q_{yy} = −29.5, Q_{zz} = 10.2 D·Å, see Table S1 for details), making the $TCNB^-$ anion an ideal system to search for an excited QBS. Theoretical calculations have indeed suggested such a weakly-bound QBS with A_g symmetry below the detachment threshold (see the inset of Figure 1 for the QBS orbital and Supporting Information for details of the calculations). Furthermore, unlike other highly symmetric systems such as C_{60} whose anion is distorted due to the Jahn−Teller effect,[45] the $TCNB^-$ anion has the same D_{2h} symmetry as neutral TCNB, making symmetry selection rules of vibronic transitions strictly obeyed.

RESULTS AND DISCUSSION

Photoelectron Spectroscopy. The experiment was performed using an electrospray-PES apparatus[46] equipped with a cryogenically cooled Paul trap[47] and a high-resolution photoelectron (PE) imaging system[48] (see Supporting Information for more details). We first measured the nonresonant PE spectra of $TCNB^-$ at two photon energies, as shown in Figure S1. The peak 0_0^0 labeled in Figure S1b corresponds to the 0−0 detachment transition from the vibrational ground state of $TCNB^-$ to that of neutral TCNB. The binding energy of peak 0_0^0 is 2.4695 ± 0.0025 eV (19 918 ± 20 cm^{-1}) representing the adiabatic electron affinity (EA) of TCNB, which was not accurately known before.[43,44] Numerous well-resolved vibrational peaks (labeled as A−D and a−e) are observed in the higher resolution spectrum (Figure 1b), and they can be assigned (Table S2) using the calculated harmonic frequencies for TCNB (Table S3). A Franck−Condon (FC) simulation for the ground state transition is compared with the spectrum in Figure S1a. The structural changes between the anion and neutral ground states are shown in Figure S1c.

Photodetachment Spectroscopy. To search for the QBS of $TCNB^-$, we measured the photodetachment spectrum by monitoring the total electron yield as a function of photon energy across the detachment threshold (Figure 1). The arrow at 19 918 cm^{-1} indicates the detachment threshold of $TCNB^-$, as mentioned above from peak 0_0^0 in the PE spectrum (Figure S1b). Eleven below-threshold vibrational peaks (labeled 1−11) and eight above-threshold peaks, i.e., vibrational Feshbach resonances (labeled 12−19) are identified (see Table S4 for their wavelengths and excitation energies). The rising baseline above the detachment threshold is due to nonresonant one-photon detachment processes, while the resonant peaks should correspond to the vibrational levels of the expected QBS. Since no more peaks were observed below peak 1, it was tempting to assume that peak 1 should represent the ground vibrational level of the QBS. All other peaks should then be due to higher vibrational levels of the QBS, and they should be assigned by comparing their relative shifts to peak 1 with the theoretical frequencies of the neutral TCNB (Table S3). Under this assumption, however, none of the observed peaks could be assigned to any vibrational levels of TCNB, suggesting that peak 1 might not represent the ground vibrational level of the QBS; i.e., the true vibrational ground state of the QBS was not observed in the photodetachment spectrum of Figure 1.

It should be noted that the QBS has A_g symmetry and the $TCNB^-$ anion has A_u symmetry (see the inset of Figure 1 and Table S5). A symmetry analysis reveals that the transition from the A_u to A_g state is triply forbidden by the electric dipole (E1), magnetic dipole (M1), and electric quadrupole (E2) and is only allowed by the electric octupole (E3). Given such a high-order forbidden transition, we would not expect that the 0−0

https://dx.doi.org/10.1021/jacs.0c10552
J. Am. Chem. Soc. XXXX, XXX, XXX−XXX

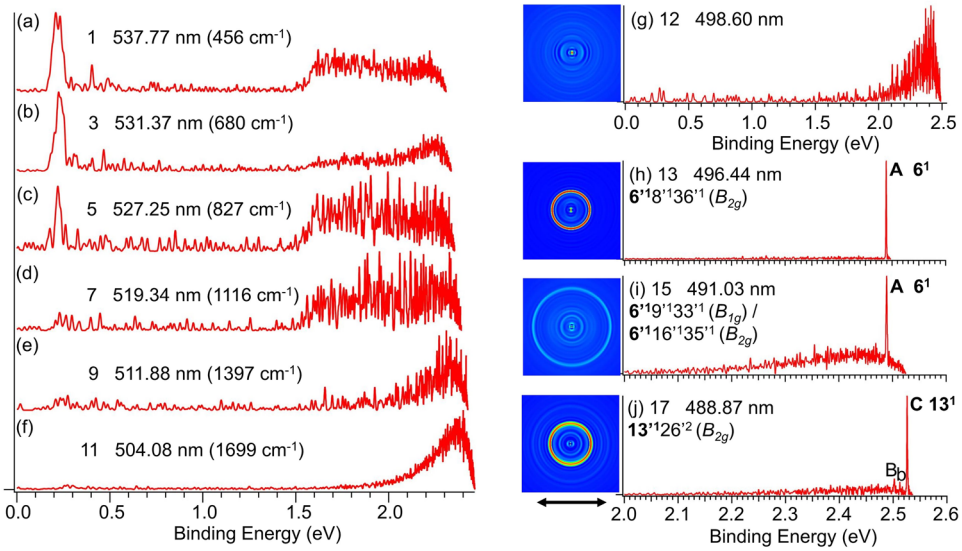

Figure 2. R2PD PE spectra of $TCNB^-$ for selected below-threshold QBS vibrational levels (a–f) and resonant PE images and spectra for selected above-threshold QBS vibrational levels (g–j). The peak numbers and excitation wavelengths are labeled. The energy shift relative to the 0–0 transition corresponding to each below-threshold vibrational peak is indicated in the parentheses in the left column. In the right column, peaks labeled in boldface with capital letters indicate autodetachment-enhanced vibrational levels in the final neutral TCNB. The assignments of the above-threshold QBS vibrational levels and their symmetries (in parentheses) are also given. The double arrow below the PE image represents the laser polarization direction.

transition from $TCNB^-$ to the QBS to be observable. However, selected higher vibrational levels of the QBS with suitable vibronic symmetries may be allowed (*vide infra*), corresponding to the observed peaks (1–19). We should note that similar vibronic selection rules are well known in Rydberg spectroscopy and vibronic transitions of neutral polyatomic molecules.[49−51]

Resonant Two-Photon Photoelectron Spectroscopy. The below-threshold vibronic levels (1–11) were observed due to resonant two-photon detachment (R2PD). By tuning the laser wavelength to these bound vibronic levels, R2PD PE spectra could be obtained, as shown in Figure 2 for six cases (left column) and Figure S2 for all 11 vibronic levels. The binding energies of the spectra were obtained by subtracting the electron kinetic energy from the photon energies used. The spectra in Figure 2a–c display a low binding energy peak at 0.22 eV, which should represent the energy difference between the detachment threshold and the intermediate QBS vibronic levels. However, the binding energy of this peak is *constant*, regardless of the vibronic levels. This observation suggests an adiabatic detachment process by the second photon, where the vibrational states in the QBS and the final neutral are not changed due to their similar geometries. In other words, if the second photon detaches the electron from the $v = n$ vibrational level of the QBS, the final neutral state would also be in the $v = n$ vibrational level. Similar adiabatic detachment processes have been reported recently for R2PD processes via DBS.[52,53] This is an important observation, suggesting that the 0.22 eV binding energy should correspond to that of the ground vibrational level of the QBS. The 0.22 eV binding energy of the QBS agrees well with the computed value of 0.16 eV (Table S5). As will be shown below, peak 1 in Figure 1 is due to the ν_{13} mode, which is observed in the PE spectrum as the most intense vibrational peak (peak C in Figure S1b). The frequency of the ν_{13} mode is measured more accurately as 456 cm^{-1} (Table S2) from the near-threshold resonant PE spectrum presented in Figure 2j (*vide infra*). This result allows us to deduce a very precise excitation energy to the ground vibrational level of the QBS (18 139 ± 8 cm^{-1}) or a binding energy of the QBS as 1779 ± 8 cm^{-1} (0.2206 ± 0.0010 eV) below the detachment threshold.

Assignments of the QBS Vibrational Levels and Their Symmetry Requirements. The deduced ground vibrational level of the QBS is indicated by the dashed arrow and the putative label 0 in Figure 1. With the determination of the vibrational ground state of the QBS, all the observed 19 vibrational peaks in the photodetachment spectrum in Figure 1 should be readily assigned using the computed frequencies of TCNB (Table S3) and the proper vibronic symmetries. Symmetry analyses for the excited vibrational levels of the QBS suggest that only transitions to vibrational (vibronic) states of the QBS with B_{1g}, B_{2g}, or B_{3g} symmetries are dipole-allowed (see the Supporting Information). Therefore, all the vibrational peaks observed in Figure 1 should correspond to vibrational levels with B_{1g}, B_{2g}, or B_{3g} symmetries. For example, peak 1 is 456 cm^{-1} above the QBS ground state, which is in excellent agreement with the calculated frequency of mode ν_{13}' (456 cm^{-1}, Table S3) of the QBS with B_{2g} symmetry. Peaks 2 and 3 are assigned to the ν_{18}' (B_{1g}) and ν_{20}' (B_{3g}) modes, respectively, again in excellent agreement with the computed frequencies and the expected vibronic symmetries (Tables S3 and S4). Similarly, other peaks can be assigned to vibrational levels of the QBS with B_{1g}, B_{2g}, or B_{3g} symmetries, as summarized in Table S4, which shows that all the higher energy peaks (4–19) correspond to combinational vibrational levels. In most cases, more than one assignment was possible due to the large number of low frequency modes and the increased vibrational density of states. It should be pointed out that the symmetry constraint has greatly simplified the photodetachment spectrum of $TCNB^-$ in Figure 1. For example, we observed 46 DBS vibrational peaks in the photodetachment spectrum of deprotonated uracil anion ($C_4H_3N_2O_2^-$) with 11 atoms in an energy range only 1800 cm^{-1} above the DBS ground state.[54] The $TCNB^-$ ($C_{10}H_2N_4^-$) anion with 16 atoms should have a

https://dx.doi.org/10.1021/jacs.0c10552
J. Am. Chem. Soc. XXXX, XXX, XXX−XXX

much higher vibrational density of states than $C_4H_3N_2O_2^-$, but within 1800 cm^{-1} above the ground state of the QBS, only 11 vibrational peaks were observed.

Intramolecular Vibrational Energy Redistribution and Radiative Processes from the QBS. The 0.22 eV R2PD PE peak is much weaker in Figure 2d–f. In all the R2PD spectra (Figure S2), broad and continuous signals were observed in the high binding energy side, implying other relaxation processes following the first photon absorption. Two types of signals were observed. The feature in Figure 2e and Figure 2f rises with increasing binding energies (lowering kinetic energies) and is peaked at the highest binding energy. This behavior suggests that the second photon detaches an electron from the vibrational manifold of $TCNB^-$ in its ground electronic state, due to internal conversion (IC) from the QBS and subsequent intramolecular vibrational energy redistributions (IVRs).[55,56] In Figure 2a–d, the broad feature has an onset around 1.55 eV, indicating electron detachment from an electronically excited state of $TCNB^-$.[52] Interestingly, the observed onset binding energy is in good agreement with the theoretical prediction of a valence excited state (VES) at a binding energy of 1.55 eV with B_{1u} symmetry (Table S5). The sharp onset of this feature suggests that the population of the VES should come from a radiative process from the QBS, following the first photon absorption.[52] It appears that the IC-IVR and the radiative process are competing and depend on the specific vibrational levels of the QBS. In Figure 2e and Figure 2f, the IC-IVR dominates, whereas in Figure 2a–d the radiative process is more favored. Figure S2 shows that most of the below-threshold vibrational levels of the QBS favor the radiative process.

Resonant Photoelectron Spectroscopy and Vibrational Autodetachment from the QBS. By tuning the detachment laser to the vibrational Feshbach resonances (12–19), eight resonantly-enhanced PE images and spectra were obtained (Figure S3), four of which are presented in Figure 2g–j. As discussed previously,[13–16,41] two processes contribute to the rPES signals: (1) the nonresonant direct detachment represented by the above-threshold baseline in Figure 1 and (2) the much stronger vibrational autodetachment that gave rise to the resonant peaks (12–19). Figure S3 indicates that the nonresonant PE signals were very weak, only observable in Figure S3e–h. The vibrational autodetachment is a two-step process. First, the $TCNB^-$ anion is excited to an above-threshold vibrational level of the QBS. Then, vibronic coupling transfers the vibrational energy to the quadrupole-bound electron to detach it into the continuum. The vibrational autodetachment enhances the intensities of certain vibrational peaks, resulting in highly non-Franck–Condon PE spectra. If there is little geometry change from the QBS to neutral TCNB, the autodetachment is expected to obey the $\Delta v = -1$ propensity rule under the harmonic approximation,[57,58] as has been shown for both DBS and QBS previously.[13–16,41] Violations of the $\Delta v = -1$ propensity rule have been observed due to anharmonic effects. Note that the QBS vibrational levels must also have the proper symmetries (B_{1g}, B_{2g}, or B_{3g}). For example, Figure 2j is assigned as an excitation to the $13'^{1}26'^{2}$ vibrational levelof the QBS (B_{2g} symmetry), followed by the transfer of the two quanta vibrational energies in $26'^{2}$ to the quadrupole-bound electron to result in the enhancement of the 13^1 final state in the PE spectra. Figure 2h and Figure 2i and the rest of the resonant PE spectra in Figure S3 can be understood similarly. The resonant PE spectra allow us to accurately measure the vibrational frequencies of the enhanced modes (see Table S2). Note that the highly accurate ν_{13} frequency is used to deduce the precise binding energy of the QBS as discussed above, because peak 1 in the photodetachment spectrum (Figure 1) is due to the same ν_{13} mode in the QBS. A broad PE feature is also observed in Figure 2i (and Figure 2j to a lesser extent), similar to that in Figure 2e and Figure 2f, suggesting that IC-IVR is competing with autodetachment in the above-threshold vibrational levels of the QBS. An extreme case is observed in Figure 2g, where no vibrational autodetachment was observed and IC-IVR seemed to be completely dominating. Since the excited QBS vibrational level (peak **12**) is just above the detachment threshold only by 138 cm^{-1} (Figure 1), this observation suggests the existence of a potential barrier, which suppresses the near-threshold autodetachment. As described in the Supporting Information and Figure S4, the centrifugal interaction $[l(l+1)/r^2]$ and the attractive quadrupolar potential $(-1/r^3)$ can indeed produce a potential barrier for the outgoing electron with a nonzero angular momentum ($l > 0$).

Figure 3 displays a schematic energy level diagram showing autodetachment from three excited QBS vibrational levels to vibrational levels of the neutral TCNB (corresponding to Figure 2h–j) and the suppression of autodetachment by a centrifugal barrier (Figure 2g). Different relaxation mechanisms from the QBS to the anion ground state and a VES are also indicated. A complete energy level diagram showing all the

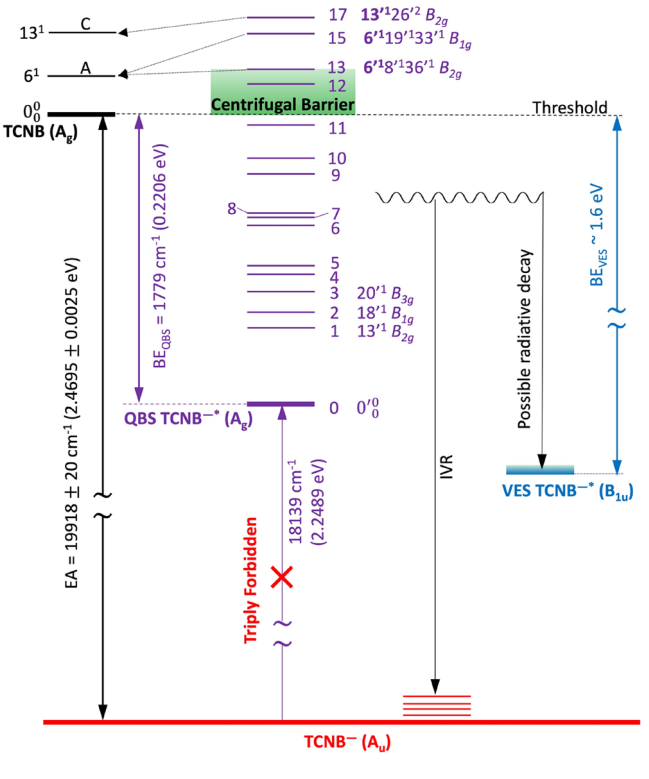

Figure 3. A schematic energy level diagram showing the autodetachment from the QBS vibrational levels of $TCNB^-$ to the neutral vibrational manifold of TCNB (left). The possible radiative decay to the VES and relaxation to the vibrational manifold of the anion ground state via IVR (right), as well as the centrifugal barrier in the near above-threshold region (middle), are also shown. See Figure S5 for a more complete diagram.

https://dx.doi.org/10.1021/jacs.0c10552
J. Am. Chem. Soc. XXXX, XXX, XXX–XXX

observed QBS vibrational levels can be found in Figure S5. By combining the photodetachment spectroscopy and the resonant and nonresonant PE spectra, we obtained the fundamental vibrational frequencies for nine vibrational modes of TCNB, as summarized in Table S6.

Evidence of Electron Correlation and Polarization Effects in the QBS. The observed binding energy (0.2206 eV) of the QBS in $TCNB^-$ is quite large in comparison to that of the recently reported quadrupole-bound anions,[39,40] suggesting the importance of electron correlation and polarization in the electron binding in the QBS. The term QBS is largely from consideration of the one-particle model potential using multiple expansion of the electrostatic interactions. It has been recognized that electron correlation plays a central role in the electron binding in all noncovalence states.[8,23,28,38,59−61] In the case of QBS, such multielectron effects are even more critical.[28,38] For TCNB, the large polarizability of the aromatic π system is also expected to be important for the electron binding. Thus, TCNB provides an interesting system to investigate the different effects to the binding of the nonvalence state, in addition to the symmetry selection rules. We computed the binding energy of the QBS at the Hartree−Fock level using the aug-cc-pvdz+4s3p2d basis set and obtained a value of 0.007 eV, indicating the importance of the quadrupolar interaction. We expect that a basis set with more diffuse functions should yield an even higher binding energy for the QBS. We should point out that a nonvalence state was predicted for hexafluorobenzene (C_6F_6) with a large binding energy and it was viewed as a correlation-bound state.[62] However, the magnitude of the quadrupole moment of C_6F_6 ($Q_{xx} = -3.2$, $Q_{yy} = -3.2$, $Q_{zz} = 6.4$) is significantly smaller than that of $TCNB^-$ (Table S1). Hence, we think the nonvalence state in $TCNB^-$ should be viewed as a QBS with strong correlation and polarization effects. It should be noted that recently a similar anion, tetracyanoethylene ($TCNE^-$), has been studied theoretically and predicted to have a nonvalence excited state with a binding energy of 0.07 eV.[61] The smaller binding energy for the QBS in $TCNE^-$ is consistent with its smaller size and lower polarizability in comparison to that of TCNB.

CONCLUSIONS

We report the observation of an excited quadrupole-bound state in the negative ion of TCNB, which forms a stable valence anion with an electron binding energy of 2.4695 eV. The QBS is 0.2206 eV below the detachment threshold of $TCNB^-$, but the transition from the ground vibrational state of $TCNB^-$ to that of the QBS is E1, M1, and E2 triply forbidden due to the high symmetry of the system (D_{2h}). Only transitions to selected vibrational levels of the QBS with B_{1g}, B_{2g}, or B_{3g} symmetries are dipole-allowed, yielding a relatively simply photodetachment spectrum. A centrifugal barrier is found to suppress autodetachment for the near-threshold vibrational Feshbach resonance. Both internal conversion and relaxation to a low-lying valence excited state were observed from the QBS. The current work reports a rare case where symmetry-selection rules are observed to be critical for vibronic transitions from a valence to a nonvalence state in a molecular anion.

ASSOCIATED CONTENT

Supporting Information

The Supporting Information is available free of charge at https://pubs.acs.org/doi/10.1021/jacs.0c10552.

Experimental and computational details, group theoretical analysis, and additional tables and figures (PDF)

AUTHOR INFORMATION

Corresponding Author

Lai-Sheng Wang − *Department of Chemistry, Brown University, Providence, Rhode Island 02912, United States;* orcid.org/0000-0003-1816-5738; Email: Lai-Sheng_Wang@brown.edu

Authors

Yuan Liu − *Department of Chemistry, Brown University, Providence, Rhode Island 02912, United States*

Guo-Zhu Zhu − *Department of Chemistry, Brown University, Providence, Rhode Island 02912, United States*

Dao-Fu Yuan − *Department of Chemistry, Brown University, Providence, Rhode Island 02912, United States;* orcid.org/0000-0001-8461-6889

Chen-Hui Qian − *Department of Chemistry, Brown University, Providence, Rhode Island 02912, United States*

Yue-Rou Zhang − *Department of Chemistry, Brown University, Providence, Rhode Island 02912, United States*

Brenda M. Rubenstein − *Department of Chemistry, Brown University, Providence, Rhode Island 02912, United States*

Complete contact information is available at: https://pubs.acs.org/10.1021/jacs.0c10552

Notes

The authors declare no competing financial interest.

ACKNOWLEDGMENTS

This work was supported by the U.S. Department of Energy, Office of Basic Energy Sciences, Chemical Sciences, Geosciences, and Biosciences Division under Grant DESC0018679. We thank Professors Richard Stratt and Peter Weber for stimulating discussions. Y.L. was supported by the Brown Presidential Fellowship. The calculation was done using computational resources and services provided by the Center for Computation and Visualization at Brown University.

REFERENCES

(1) Fermi, E.; Teller, E. The capture of negative mesotrons in matter. *Phys. Rev.* **1947**, *72*, 399−408.

(2) Turner, J. E. Minimum dipole moment required to bind an electron—molecular theorists rediscover phenomenon mentioned in Fermi-Teller paper twenty years earlier. *Am. J. Phys.* **1977**, *45*, 758−766.

(3) Desfrancois, C.; Abdoul-Carime, H.; Schermann, J. P. Ground-state dipole-bound anions. *Int. J. Mod. Phys. B* **1996**, *10*, 1339.

(4) Desfrancois, C.; Abdoulcarime, H.; Khelifa, N.; Schermann, J. P. From 1/r to $1/r^2$ potentials: Electron exchange between Rydberg atoms and polar molecules. *Phys. Rev. Lett.* **1994**, *73*, 2436−2439.

(5) Hammer, N. I.; Diri, K.; Jordan, K. D.; Desfrancois, C.; Compton, R. N. Dipole-bound anions of carbonyl, nitrile, and sulfoxide containing molecules. *J. Chem. Phys.* **2003**, *119*, 3650−3660.

(6) Hammer, N. I.; Hinde, R. J.; Compton, R. N.; Diri, K.; Jordan, K. D.; Radisic, D.; Stokes, S. T.; Bowen, K. H. Dipole-bound anions of

highly polar molecules: Ethylene carbonate and vinylene carbonate. *J. Chem. Phys.* **2004**, *120*, 685−690.
(7) Jordan, K. D.; Wang, F. Theory of dipole-bound anions. *Annu. Rev. Phys. Chem.* **2003**, *54*, 367−396.
(8) Qian, C. H.; Zhu, G. Z.; Wang, L. S. Probing the critical dipole moment to support excited dipole-bound states in valence-bound anions. *J. Phys. Chem. Lett.* **2019**, *10*, 6472−6477.
(9) Stockdale, J. A.; Davis, F. J.; Compton, R. N.; Klots, C. E. Production of negative ions from CH_3X molecules (CH_3NO_2, CH_3CN, CH_3I, CH_3Br) by electron impact and by collisions with atoms in excited Rydberg states. *J. Chem. Phys.* **1974**, *60*, 4279−4285.
(10) Zimmerman, A. H.; Brauman, J. I. Resonances in electron photodetachment cross sections. *J. Chem. Phys.* **1977**, *66*, 5823−5825.
(11) Lykke, K. R.; Mead, R. D.; Lineberger, W. C. Observation of dipole-bound states of negative ions. *Phys. Rev. Lett.* **1984**, *52*, 2221−2224.
(12) Mead, R. D.; Lykke, K. R.; Lineberger, W. C.; Marks, J.; Brauman, J. I. Spectroscopy and dynamics of the dipole-bound state of acetaldehyde enolate. *J. Chem. Phys.* **1984**, *81*, 4883−4892.
(13) Liu, H. T.; Ning, C. G.; Huang, D. L.; Dau, P. D.; Wang, L. S. Observation of mode-specific vibrational autodetachment from dipole-bound states of cold anions. *Angew. Chem., Int. Ed.* **2013**, *52*, 8976−8979.
(14) Huang, D. L.; Liu, H. T.; Ning, C. G.; Wang, L. S. Vibrational state-selective autodetachment photoelectron spectroscopy from dipole-bound states of cold 2-hydroxyphenoxide: *o*-$HO(C_6H_4)O^-$. *J. Chem. Phys.* **2015**, *142*, 124309.
(15) Zhu, G. Z.; Huang, D. L.; Wang, L. S. Conformation-selective resonant photoelectron imaging from dipole-bound states of cold 3-hydroxyphenoxide. *J. Chem. Phys.* **2017**, *147*, 013910.
(16) Zhu, G. Z.; Wang, L. S. High-resolution photoelectron imaging and resonant photoelectron spectroscopy via noncovalently bound excited states of cryogenically cooled anions. *Chem. Sci.* **2019**, *10*, 9409−9423.
(17) Dao, D. B.; Mabbs, R. The effect of the dipole bound state on AgF^- vibrationally resolved photodetachment cross sections and photoelectron angular distributions. *J. Chem. Phys.* **2014**, *141*, 154304.
(18) Lyle, J.; Wedig, O.; Gulania, S.; Krylov, A. I.; Mabbs, R. Channel branching ratios in CH_2CN^- photodetachment: Rotational structure and vibrational energy redistribution in autodetachment. *J. Chem. Phys.* **2017**, *147*, 234309.
(19) Mascaritolo, K. J.; Dermer, A. M.; Green, M. L.; Gardner, A. M.; Heaven, M. C. Photodetachment spectroscopy of the beryllium oxide anion, BeO^-. *J. Chem. Phys.* **2017**, *146*, 054301.
(20) Castellani, M. E.; Anstoter, C. S.; Verlet, J. R. R. On the stability of a dipole-bound state in the presence of a molecule. *Phys. Chem. Chem. Phys.* **2019**, *21*, 24286−24290.
(21) Kang, D. H.; An, S.; Kim, S. K. Real-time autodetachment dynamics of vibrational Feshbach resonances in a dipole-bound state. *Phys. Rev. Lett.* **2020**, *125*, 093001.
(22) Compton, R. N.; Hammer, N. I. In *Advances in Gas-Phase Ion Chemistry*; Adams, N., Babcock, I., Eds.; Elsevier Science: New York, 2001; pp 257−305.
(23) Simons, J. Molecular anions. *J. Phys. Chem. A* **2008**, *112*, 6401−6511.
(24) Prasad, M. V. N. A.; Wallis, R. F.; Herman, R. Theory of the binding energy of an electron in the field of a linear electric quadrupole. *Phys. Rev. B: Condens. Matter Mater. Phys.* **1989**, *40*, 5924−5928.
(25) Abdoul-Carime, H.; Desfrancois, C. Electrons weakly bound to molecules by dipolar, quadrupolar or polarization forces. *Eur. Phys. J. D* **1998**, *2*, 149−156.
(26) Ferron, A.; Serra, P.; Kais, S. Finite-size scaling for critical conditions for stable quadrupole-bound anions. *J. Chem. Phys.* **2004**, *120*, 8412−8419.
(27) Garrett, W. R. Quadrupole-bound anions: Efficacy of positive versus negative quadrupole moments. *J. Chem. Phys.* **2012**, *136*, 054116.
(28) Sommerfeld, T.; Dreux, K. M.; Joshi, R. Excess electrons bound to molecular systems with a vanishing dipole but large molecular quadrupole. *J. Phys. Chem. A* **2014**, *118*, 7320−7329.
(29) Jordan, K. D.; Liebman, J. F. Binding of an electron to a molecular quadrupole: $(BeO)_2$. *Chem. Phys. Lett.* **1979**, *62*, 143−147.
(30) Gutsev, G. L.; Jena, P.; Bartlett, R. J. Search for "quadrupole-bound" anions. I. *J. Chem. Phys.* **1999**, *111*, 504−511.
(31) Anusiewicz, I.; Skurski, P.; Simons, J. First evidence of rhombic $(NaCl)_2^-$. Ab initio reexamination of the sodium chloride dimer anion. *J. Phys. Chem. A* **2002**, *106*, 10636−10644.
(32) Gutowski, M.; Skurski, P.; Li, X.; Wang, L. S. $(MgO)_n^-$ (n = 1-5) clusters: Multipole-bound anions and photodetachment spectroscopy. *Phys. Rev. Lett.* **2000**, *85*, 3145−3148.
(33) Desfrancois, C.; Khelifa, N.; Schermann, J. P.; Kraft, T.; Ruf, M. W.; Hotop, H. Energy exchanges following very low energy electron attachment to neat CS_2 and CS_2-containing clusters. *Z. Phys. D: At., Mol. Clusters* **1993**, *27*, 365−369.
(34) Compton, R. N.; Dunning, F. B.; Nordlander, P. On the binding of electrons to CS_2: Possible role of quadrupole-bound states. *Chem. Phys. Lett.* **1996**, *253*, 8−12.
(35) Desfrancois, C.; Periquet, V.; Carles, S.; Schermann, J. P.; Adamowicz, L. Neutral and negatively-charged formamide, N-methylformamide and dimethylformamide clusters. *Chem. Phys.* **1998**, *239*, 475−483.
(36) Desfrancois, C.; Periquet, V.; Lyapustina, S. A.; Lippa, T. P.; Robinson, D. W.; Bowen, K. H.; Nonaka, H.; Compton, R. N. Electron binding to valence and multipole states of molecules: Nitrobenzene, para- and meta-dinitrobenzenes. *J. Chem. Phys.* **1999**, *111*, 4569−4576.
(37) Desfrancois, C.; Bouteiller, Y.; Schermann, J. P.; Radisic, D.; Stokes, S. T.; Bowen, K. H.; Hammer, N. I.; Compton, R. N. Long-range electron binding to quadrupolar molecules. *Phys. Rev. Lett.* **2004**, *92*, 083003.
(38) Sommerfeld, T. Multipole-bound states of succinonitrile and other dicarbonitriles. *J. Chem. Phys.* **2004**, *121*, 4097−4104.
(39) Liu, G.; Ciborowski, S. M.; Graham, J. D.; Buytendyk, A. M.; Bowen, K. H. The ground state, quadrupole-bound anion of succinonitrile revisited. *J. Chem. Phys.* **2019**, *151*, 101101.
(40) Liu, G.; Ciborowski, S. M.; Pitts, C. R.; Graham, J. D.; Buytendyk, A. M.; Lectka, T.; Bowen, K. H. Observation of the dipole-and quadrupole-bound anions of 1, 4-dicyanocyclohexane. *Phys. Chem. Chem. Phys.* **2019**, *21*, 18310−18315.
(41) Zhu, G. Z.; Liu, Y.; Wang, L. S. Observation of excited quadrupole-bound states in cold anions. *Phys. Rev. Lett.* **2017**, *119*, 023002.
(42) Campanelli, A. R.; Domenicano, A.; Ramondo, F.; Hargittai, I. Molecular structure and benzene ring deformation of three cyanobenzenes from gas-phase electron diffraction and quantum chemical calculations. *J. Phys. Chem. A* **2008**, *112*, 10998−11088.
(43) Farragher, A. L.; Page, F. M. Experimental determination of electron affinities. Part 11.—Electron capture by some cyanocarbons and related compounds. *Trans. Faraday Soc.* **1967**, *63*, 2369−2378.
(44) Nakashima, H.; Honda, Y.; Shida, T.; Nakatsuji, H. Electronic excitation spectra of doublet anion radicals of cyanobenzene and nitrobenzene derivatives: SAC-CI theoretical studies. *Mol. Phys.* **2015**, *113*, 1728−1739.
(45) Huang, D. L.; Dau, P. D.; Liu, H. T.; Wang, L. S. High-resolution photoelectron imaging of cold C_{60}^- anions and accurate determination of the electron affinity of C_{60}. *J. Chem. Phys.* **2014**, *140*, 224315.
(46) Wang, L. S. Perspective: Electrospray photoelectron spectroscopy: From multiply-charged anions to ultracold anions. *J. Chem. Phys.* **2015**, *143*, 040901.
(47) Wang, X. B.; Wang, L. S. Development of a low-temperature photoelectron spectroscopy instrument using an electrospray ion source and a cryogenically controlled ion trap. *Rev. Sci. Instrum.* **2008**, *79*, 073108.
(48) Leon, I.; Yang, Z.; Liu, H. T.; Wang, L. S. The design and construction of a high-resolution velocity-map imaging apparatus for

https://dx.doi.org/10.1021/jacs.0c10552
J. Am. Chem. Soc. XXXX, XXX, XXX−XXX

photoelectron spectroscopy studies of size-selected clusters. *Rev. Sci. Instrum.* **2014**, *85*, 083106.
(49) Vitenberg, R.; Katz, B.; Scharf, B. The assignment of the benzene first-ionization Rydberg spectrum via J-T splittings involving linearly inactive modes. *Chem. Phys. Lett.* **1980**, *71*, 187−191.
(50) Signorell, R.; Merkt, F. General symmetry selection rules for the photoionization of polyatomic molecules. *Mol. Phys.* **1997**, *92*, 793−804.
(51) Philis, J. G.; Mondal, T.; Mahapatra, S. Vibronic structure in the low lying Rydberg states of hexafluoro-benzene and 1,3,5-trifluorobenzene detected by two-photon spectroscopy. *Chem. Phys. Lett.* **2010**, *495*, 187−191.
(52) Zhu, G. Z.; Cheung, L. F.; Liu, Y.; Qian, C. H.; Wang, L. S. Resonant two-photon photoelectron imaging and intersystem crossing from excited dipole-bound states of cold anions. *J. Phys. Chem. Lett.* **2019**, *10*, 4339−4344.
(53) Yuan, D. F.; Liu, Y.; Qian, C. H.; Kocheril, G. S.; Zhang, Y. R.; Rubenstein, B. M.; Wang, L. S. Polarization of valence orbitals by the intramolecular electric field from a diffuse dipole-bound electron. *J. Phys. Chem. Lett.* **2020**, *11*, 7914−7919.
(54) Liu, H. T.; Ning, C. G.; Huang, D. L.; Wang, L. S. Vibrational spectroscopy of the dehydrogenated uracil radical by autodetachment of dipole-bound excited states of cold anions. *Angew. Chem., Int. Ed.* **2014**, *53*, 2464−2468.
(55) Stannard, P. R.; Gelbart, W. M. Intramolecular vibrational energy redistribution. *J. Phys. Chem.* **1981**, *85*, 3592−3599.
(56) Yuan, D. F.; Liu, Y.; Qian, C. H.; Zhang, Y. R.; Rubenstein, B. M.; Wang, L. S. Observation of a π-type dipole-bound state in molecular anions. *Phys. Rev. Lett.* **2020**, *125*, 073003.
(57) Berry, R. S. Ionization of molecules at low energies. *J. Chem. Phys.* **1966**, *45*, 1228−1245.
(58) Simons, J. Propensity rules for vibration-induced electron detachment of anions. *J. Am. Chem. Soc.* **1981**, *103*, 3971−3976.
(59) Gutowski, M.; Jordan, K. D.; Skurski, P. Electronic structure of dipole-bound anions. *J. Phys. Chem. A* **1998**, *102*, 2624−2633.
(60) Voora, V. K.; Cederbaum, L. S.; Jordan, K. D. Existence of a correlation bound s-type anion state of C_{60}. *J. Phys. Chem. Lett.* **2013**, *4*, 849−853.
(61) Voora, V. K.; Kairalapova, A.; Sommerfeld, T.; Jordan, K. D. Theoretical approaches for treating non-valence correlation-bound anions. *J. Chem. Phys.* **2017**, *147*, 214114.
(62) Voora, V. K.; Jordan, K. D. Nonvalence correlation-bound state of C_6F_6: doorways to low-energy electron cpature. *J. Phys. Chem. A* **2014**, *118*, 7201−7205.

https://dx.doi.org/10.1021/jacs.0c10552
J. Am. Chem. Soc. XXXX, XXX, XXX−XXX